Numerical Analysis on the Discharge Characteristics of a Liquid Rocket Engine Injector Orifice

Won Kook Cho* and Young-Mog Kim**
Rocket Engine Research Department
Korea Aerospace Research Institute, Taejon, Korea 305-333

Abstract

A numerical analysis was performed on the fluid flow in injector orifice of a liquid rocket engine. The present computational code was verified against the published data for turbulent flow in a pipe with a sudden expansion-contraction. Considered were the parameters for the flow analysis in an injector orifice: Reynolds number, ratio of mass flow rate of the injector orifice and inlet flow rate, and slant angle of the injector orifice. The discharge coefficient increased slightly as the Reynolds number increased. The slant angle of the injector changed critically the discharge coefficient. The discharge coefficient increased by 7% when the slant angle changed from -30° to 30°. The ratio of mass flow rate had relatively little impact on the discharge coefficient.

Key Word : liquid rocket engine, injector orifice, discharge coefficient

Introduction

The injector of a liquid rocket engine accelerates the propellant velocity with differential pressure for atomizing and mixing in the combustion chamber. The propellant supplied through the injector should be highly homogeneous, maintain uniform mixture ratio and be readily vaporized for efficient combustion[1,2]. The impinging type, non-impinging type, splash-plate type, sheet type and premixed type are the examples of injectors. In the impinging type injector, the liquid-phase propellant goes through separated multiple passages and collide together to atomize. A sketch of propellant manifold of a liquid rocket engine with propellant injection element is given in Fig. 1.

A general purpose tool, in spite of considerable effort[3-7], has not yet been developed for injector design leaving the design process dependant on empirical or intuitive procedures. The previous researches are done mostly about the spray and mixing performance[6] of the injectors. However, little has been done on the hydrodynamic characteristics, i.e., discharge performance[4,5,7], pressure losses for the development of propellant injectors and/or manifolds. So the flow analysis of a more realistic flow model is needed to develop a new liquid rocket injectors as most previous studies deal over-simplified numerical model: laminar[4,5] or axi-symmetric flow.

The present paper presents the solution of three dimensional turbulent flow in the propellant injector orifice of a liquid rocket, KSR-III (Korea Sounding Rocket III)[8], to meet the aforementioned demands. The major parameters governing the injector orifice performance are propellant, material property, orifice size, transient flow conditions, characteristics of fluid dynamics and heat transfer, combustion instability[2]. The effect of the following parameters to the discharge coefficient is presented: Reynolds number, orifice slant angle and the ratio of orifice flow rate and the inlet flow rate.

* Senior Research Engineer
E-mail : wkcho@kari.re.kr, TEL : 042-860-2937, FAX : 042-860-2602
** Head

Nomenclature

A	area
$\mathbf{b}$	body force
C_d	discharge coefficient
C_μ	empirical coefficient of turbulence model
d	orifice diameter
$\boldsymbol{D}$	deformation rate tensor
$\boldsymbol{I}$	unit tensor
k	turbulent kinetic energy
l	turbulence length scale
p	pressure
Q	volume flow rate
Re	Reynolds number
r_m	ratio of mass flow rate
S_ϕ	source term of arbitrary scalar
$\boldsymbol{T}$	stress tensor
$\boldsymbol{v}$	velocity vector
x, y, z	coordinate
Δ	difference
ε	dissipation rate
ϕ	arbitrary scalar
Γ	diffusion coefficient
μ	dynamic viscosity
θ	orifice slant angle
ρ	density

subscripts

in	value at inlet
inj	value of injector orifice
out	value at outlet

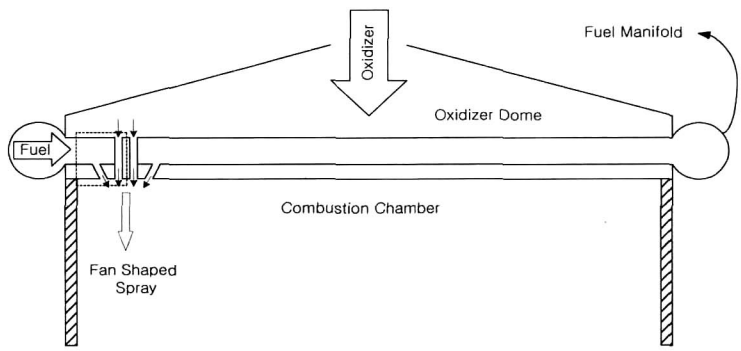

Fig. 1. Schematic of a propellant injection system of a liquid rocket engine.

The computational domain representing the flow area of a single injector is presented in a dotted rectangle in Fig. 1. The approach that a single injector represents the whole injector face assumes the curvature effect in the injector array is negligible to the discharge performance because the pressure drop of the orifice is dominant. Also assumed is uniform injection velocity regardless of the injector position[8] to compare the discharge performance for a given fixed Reynolds number. It is also based on the fact that the pressure drop through the orifice is much greater than the other losses and will be presented as a part of the result in the following section.

Numerical Methods

The governing equations are steady state three dimensional Navier-Stokes equations for incompressible flow as the Mach number is much less than unit at the injector orifice where the velocity accelerates the most, e.g., 20 to 30 m/s. The governing equations[9] which are nondimensionalized by the average orifice velocity and the orifice diameter are given as

$$\mathrm{div}\,(\rho \boldsymbol{v}) = 0 \tag{1}$$

$$\mathrm{div}\,(\rho \boldsymbol{v}\boldsymbol{v}) = \mathrm{div}\,\mathbf{T} + \rho \mathbf{b} \tag{2}$$

$$\text{div}\,(\rho\phi\boldsymbol{v}) = \text{div}\,(\Gamma\,\text{grad}\,\phi) + S_\phi \tag{3}$$

The source terms of the scalar equations are composed of turbulence generation, dissipation rate and etc. as the standard k-ε model (see reference 10 for detailed description) is adopted for turbulence. The stress tensor is given in terms of velocity vectors and pressure for the Newtonian fluid.

$$\mathbf{T} = -(p + \frac{2}{3}\mu\,\text{div}\,\boldsymbol{v})\mathbf{I} + 2\mu\mathbf{D} \tag{4}$$

The finite volume method is adopted to integrate the partial differential equation over the finite volumes. The accurate and stable QUICK scheme[11] is used for the convection terms of the momentum equations, and central difference is used for the diffusion terms. Highly stable upwind scheme differences the convection terms of the turbulence variables because the source terms, i.e., generation and dissipation, play a dominant role in turbulence phenomena[12].

Followings are the boundary conditions: the flow enters perpendicularly at the inlet with uniform velocity. The turbulence intensity is 10% of the average inlet velocity. The dissipation rate at the inlet is calculated by the following correlation

$$\varepsilon_{in} = C_\mu^{0.75}\, k_{in}^{1.5} \,/\, l \tag{5}$$

The mass flow rate at the outlet is considered to be 80%, 90% and 95% of the inlet flow rate. The above condition simulates for the 5th-, 10th- and 20th-row injector orifice respectively among the total 20-row injector orifice array. The corresponding flow rates through the orifice are 20%, 10% and 5% of the total flow rate. The outlet condition which extrapolates the distribution of the dependant variables from the results of the domain maintaining the fixed known flow rate is given as the orifice exit boundary condition.

The computational grid is shown in Fig. 2 with the boundary condition descriptions. All surfaces in the figure are no-slip solid wall if not specified. The flow enters from the bottom and the major part goes out through the top surface, and the remaining exits through the injector orifice. About the size of the flow domain, excluding the orifice injector, the height is 28.48 d_{inj}, and both the width and the length are 14.24 d_{inj}.

The ratio of the flow rate through the orifice and the bottom boundary considered as an important parameter is defined as

$$r_m = \frac{dQ}{Q_{in}} \tag{6}$$

where the flow rate through the orifice, $dQ = Q_{in} - Q_{out}$.

The following expression defines the Reynolds number which has the same sense with the flow rate once the working fluid is fixed.

$$Re = \frac{\rho\, v_{inj}\, d_{inj}}{\mu} \tag{7}$$

The working fluid, kerosene has the following property: ρ=800 kg/m^3 and μ=0.00207 kg/m·s. The material property, however, has little meaning as the present paper is a nondimensional parametric study.

The orifice slant angle shown in Fig. 2 is the angle between the orifice flow direction and the

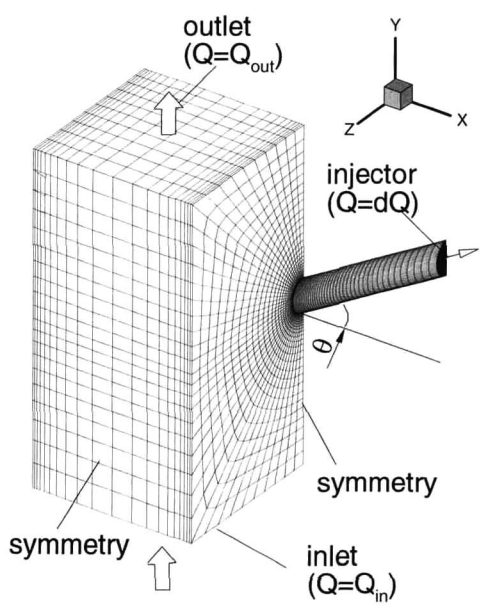

Fig. 2. Computational grid with boundary conditions.

direction perpendicular to the main flow - longitudinal direction of combustion chamber. It plays an important role in the combustion efficiency and stability as it determines the propellant spray fan pattern[2]. This also affects critically the heat transfer at the injection face because the flame location is a function of the propellant impinging point.

The present numerical procedure solves iteratively the governing equations and stops the iteration when the residual of each variable is less than 10^{-3}. Simultaneously confirmed is the state that the variation of all the variables is negligibly small at a specified location. The residual is nondimensionalized by the inlet flow rate for continuity equation and by the inlet momentum rate for the momentum equation.

Results and Discussions

A numerical solution of a bench mark problem was tackled before the main analysis to validate the present code. The present analysis program which has been applied for many flow problems[8] gives the solution of a two dimensional turbulent flow in a sudden expansion-contraction circular pipe.

The pressure coefficient along the top wall of the expansion area is depicted in Fig. 3. Inset delineates the streamlines inside the flow domain of which the expansion area length is 600mm. About the inlet condition, the velocity profile and the turbulent kinetic energy distribution is given by the experimental results of Park et al.[13] The dissipation rate at the inlet is determined by using the correlation given in Jang et al.[12]. The computational grid consists of 110×60 finite volumes. The expansion area is modeled by using 70×60 finite volumes.

The pressure coefficient, normalized pressure, agrees well with the published experimental[13] and numerical[12] data. The present curve shows faster pressure recovery than the experimental results in the area $x \geq 500$mm. This can be explained by the characteristics of the numerical results with standard k-ε model which has "a tendency of underestimating the momentum transfer in the free shear layer.[12]" The above result confirms that the present numerical program with standard k-ε model solves accurately an orifice flow problem.

The computational grid for the analysis of the injector orifice flow is made of 40×40×60 (=96,000) finite volumes which is the same order as those used in the previous researches[4,5]. The grid is confirmed to give a grid independent solution. Increasing the number of the grid changes little the discharge performance (see Fig. 4). Also carried out is the convergence test; reducing the convergence criterion up to 10^{-4} gives the same results comparing the criterion of 10^{-3} case.

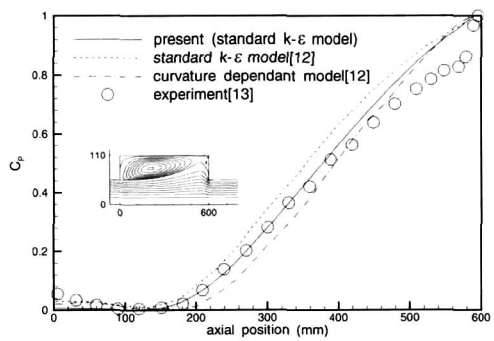

Fig. 3. Distributions of wall pressure coefficient for turbulent flows of a circular pipe with sudden expansion-contraction. Inset is the stream lines.

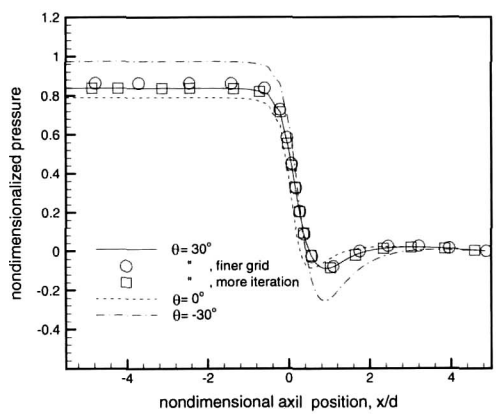

Fig. 4. Distributions of nondimensinal pressure vs. nondimensional axial position.

In Fig. 4, nondimensionalized pressure distributions are presented as a function of axial position for orifice slant angles, 30°, 0° and -30°. Other parameters are fixed, that is, Re=16,000 and m_r=0.1. In the figure, the reference position where pressure is 0 is orifice exit. Increasing the grid (48×48×86) results little difference in pressure distribution comparing with the results of the reference grid. Also confirmed is the convergence test as more iteration dose not change the results.

The dimensional pressure can be obtained from the curve by multiplying ρu_{inj}^2. For example, the unit nondimensional pressure is equivalent to 5.4×10^5pa for Re=16,000 flow in a 1.6mm-diameter orifice. The pressure is uniform in the manifold ($x\leq0$) and drops abruptly near the orifice entrance. The minimum pressure point locates right after the entrance and recovers for $x\leq2$. The feature of the pressure curve resembles that of the high Reynolds number case for laminar flow condition[4]. The pressure decreases slightly after recovery - close to constant - because of the frictional loss through the straight passage.

The pressure loss of the injector orifice is assessed by comparing the discharge coefficient defined as

$$C_d=\frac{Q_{inj}}{A\sqrt{(2\Delta p/\rho)}} \tag{8}$$

Table 1. lists the discharge coefficient vs. orifice slant angle for fixed Re=16,000 and m_r=0.1. The discharge coefficient increases slightly for small slant angle as the orifice entrance area increases with slant angle. The slant angle has more serious impacts to the discharge performance. The discharge coefficient of positive slant angle is greater by 7% than that of the negative slant angle for the considered slant angle range.

Table 1. Discharge coefficients vs. injector orifice slant angle for Re=16,000 and r_m =0.1.

θ(deg)	-40	-30	-20	0	20	30	40
C_d	0.620	0.716	0.812	0.796	0.884	0.772	0.668

Table 2. Dependance of discharge coefficient on Reynolds number and the ratio of mass flow rate.

Re	C_d	r_m	C_d
8000	0.737	0.05	0.808
16000	0.772	0.1	0.772
32000	0.782	0.2	0.757

The discharge performance is relatively insensitive to the Reynolds number and the ratio of flow rate. The influence of the Reynolds number and the ratio of the mass flow rate is summarized in Table 2. The discharge coefficient varies within 5% for the considered Reynolds number range with θ=30° and m_r=0.1. The quantitative impact of the ratio of the flow mass rate is close to that of the Reynolds number.

The velocity vectors, nondimensionalized isobars and the distribution of turbulent kinetic energy are depicted in Figs. 5 to 7 respectively for the reference case, Re=16,000, θ=30° and m_r=0.1. The velocity vectors are shown for every third row in x direction for better visibility. The working fluid flows upward (y direction) in the main flow area and turns the direction abruptly near the injector orifice. The velocity magnitude of the main flow is still less than that of the orifice. The recirculation locates at the orifice inlet due to the sudden flow direction change. After

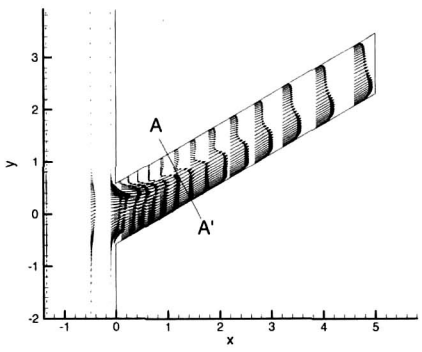

Fig. 5. Velocity vectors at symmetry plane for the reference case.

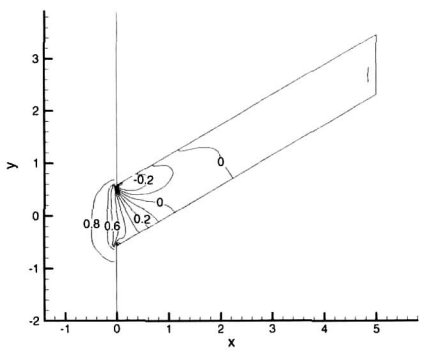

Fig. 6. Isobars at symmetry plane for the reference case.

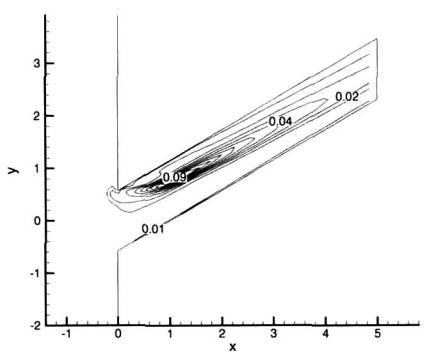

Fig. 7. Turbulent kinetic energy distribution at symmetry plane for the reference case.

this area, flow develops again, and the flow pattern resembles qualitatively with that of a laminar flow[4,5]. The flow area is categorized into two areas: one is the upper part of the orifice where low momentum is maintained, and the other is the lower area at A-A′ section where jet effect is dominant. The quantitative characteristics, however, should be different with the previous studies because the present problem is turbulent while the flow conditions of the references[4,5] are laminar. The recirculation near the orifice entrance is effectively suppressed by the secondary flow moving in z direction to restrict the recirculation area to be small. The lower pressure than neighbor induces incoming flow and strong velocity gradient, and resultantly generates highly turbulent flow.

The flow solution is given in Figs. 8 and 9 for the slant angle -30° which models the opposite side injector orifice of F-O-O-F injector element. The qualitative patterns of the flow are the same as those of the case for slant angle 30°. The enlarged angle between the main flow direction and the orifice direction generates smaller effective cross-sectional area at "vena contracta" which consequences larger pressure loss. The larger turning angle extends separation area. The pressure is lower than that of the former case in the recirculation region. Also strengthened is the turbulence level due to a steeper velocity gradient.

The quantitative comparison is definite in Figs. 10 and 11 showing the secondary flow and the axial velocity magnitude at the cross section A-A′ in Figs. 4 and 7 respectively. The secondary flow is more vigorous for the slant angle -30° case. The rotating direction is determined by the orifice slant angle; plus angle generates counter-clock-wise secondary flow whereas minus angle induces clock wise secondary flow. The axial velocity accelerates more for the negative orifice slant angle, i.e., the maximum axial velocity is 1.2 times of the average axial velocity for the slant angle 30° while it is 1.3 times for the slant angle -30°.

To summarize the effect of the orifice slant angle, the propellant injection should be directed inside (see Fig. 1 for injector orifice direction) the combustion chamber with a same slant angle, e.g., 30° and -30° for the F-O-O-F impinging injector element. The radially inward injection pattern may cause outward "radial wind[1]" at the initial combustion stage which has adverse effect to the chamber wall cooling owing to the hot gas scrubbing the chamber wall. It should be an important topic for a future study to optimize the injector orifice array for a revised injection pattern.

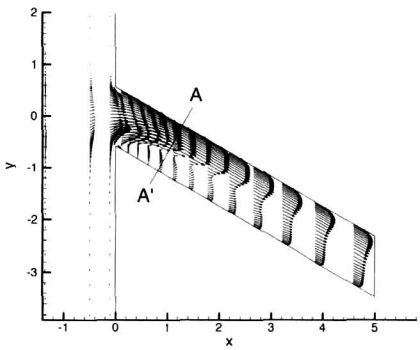

Fig. 8. Velocity vector at symmetry plane for Re=16000, θ=-30° and r_m=0.1.

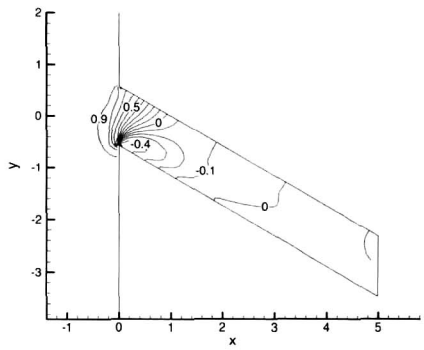

Fig. 9. Isobars at symmetry plane for Re=16000, θ=-30° and r_m=0.1.

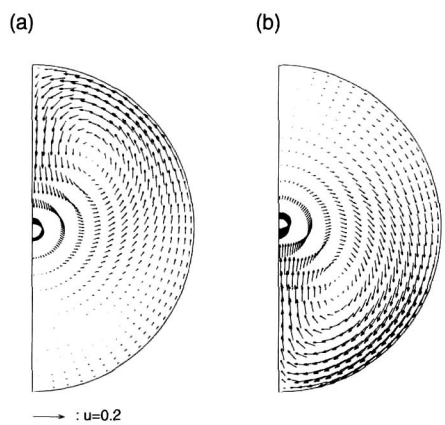

Fig. 10. Velocity vectors of secondary flow at the cross-section AA'; (a) θ=30°, (b) θ=-30°.

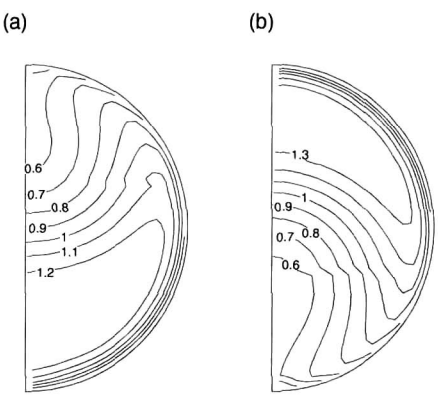

Fig. 11. Distributions of axial velocity magnitude at the cross-section AA'; (a) θ=30°, (b) θ=-30°.

Conclusions

A numerical analysis was performed for the discharge characteristics of the liquid rocket engine injector orifice. Considered parameters are: Reynolds number, orifice slant angle and ratio of mass flow rate meaning normalized orifice flow rate with respect to the total flow rate. The nondimensionalized pressure drop decreases slightly as the Reynolds number increases. Uniform injection is predicted as the discharge performance is relatively insensitive for the ratio of mass flow rate. The orifice slant angle impacts critically to the discharge characteristics. The discharge coefficient increases 7% when the slant angle changes from -30° to 30°.

Acknowledgement

The present study is a part of research efforts of KSR-III program that is supported by the Ministry of Science and Technology, Korea.

References

1. Huzel, D.K. and Huang, D.H., *Modern engineering for design of liquid-propellant rocket engines*, American Institute of Aeronautics and Astronautics, Inc., 1992.

2. Sutton, G.P. and Ross, D.M., *Elements: the engineering of rockets*, John Wiley & Sons, Inc., 1976.

3. Gill, G.S. and Nurick, W.H., *Liquid rocket engine injectors*, NASA Space Vehicle Design Criteria (Chemical), NASA SP-8089, NASA Lewis Research Center, Mar 1976.

4. Kim, Y.-M. and Oh, S.-H., "Computations of the three-dimensional flow field in a tube with sudden contraction (in Korean)," *J. of the Korean Society Aeronautical Space Sciences*, Vol. 25, No. 1, 1997, pp.25-34.

5. Kim, Y.-M., "Numerical study on the characteristics of the flow through injector orifice by multi-block computations (in Korean)," *Trans. Korea Soc. Mech. Engng. B,* Vol. 21, No. 3, 1997, pp.414-426.

6. Rho, B.J., Oh, J.H., Kang, S.J., Park, S.M. and Kwon, K.C., "A study on atomization characteristics of the double impinging F-O-O-F type injector with four streams for liquid rocket, (in Korean)," *J. of the Korean Society Aeronautical Space Sciences*, Vol. 27, No. 7, 1999, pp.112-120.

7. Cho, W.K., "Flow analysis in fuel injectors of a liquid rocket (in Korean)," *J. of the Korean Society of Aeronautical and Space Sciences*, Vol.28 No.8, 2000, pp.115-121.

8. Chae, Y.S. et al., *Research and development of KSR-III (III)* (in Korean), Vol. 1, Korea Aerospace Research Institute, 2000.

9. Ferziger, J.H. and Peric, M, *Computational methods for fluid dynamics*, Springer-Verlog, 1996.

10. Hur, N., Cho, W.K., Yoon, S.Y. and Kim, K.H., "A study on the development of general purpose program for the analysis of 3-D fluid flow by using a general non-orthogonal grid system (in Korean)," *Trans. Korea Soc. Mech. Engng.*, Vol. 18, No. 12, 1994, pp.3345-3356.

11. Leonard, B.P., A stable and accurate convective modelling procedure based on quadratic upstream interpolation, *Computer Methods in Applied Mechanics and Engineering*, Vol.19, 1979, pp.59-98.

12. Park, B.S., Sung, H.J. and Chung, M.K., "Experimental study on the turbulent flow field in a sudden expansion-contraction pipe joint (in Korean)," *Trans. Korea Soc. Mech. Engng.,* Vol. 13, No. 6, 1989, pp.1269-1281.

13. Jang, H.C., Sung, H.J. and Choi, H.O., "Curvature-dependent two-equation model for turbulent sudden expansion-contraction pipe joint flows (in Korean)," *Trans. Korea Soc. Mech. Engng.,* Vol. 15, No. 5, 1991, pp.1747-1755.